

# Fluorescence Ratiometric Sensor for Trace Vapor Detection of Hydrogen Peroxide

Miao Xu,<sup>†,§</sup> Ji-Min Han,<sup>†,§</sup> Chen Wang,<sup>†</sup> Xiaomei Yang,<sup>†</sup> Jian Pei,<sup>‡</sup> and Ling Zang<sup>\*,†</sup>

<sup>†</sup>Department of Materials Science and Engineering, University of Utah, 36 South Wasatch Drive, Salt Lake City, Utah 84112, United States

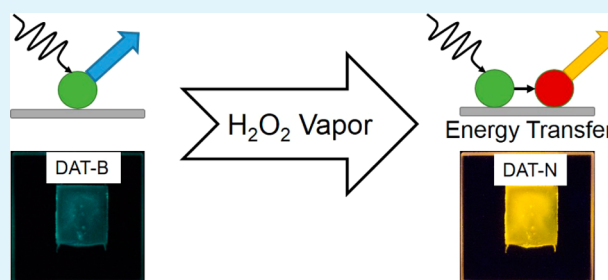
<sup>‡</sup>Beijing National Laboratory for Molecular Sciences, Key Laboratory of Bioorganic Chemistry and Molecular Engineering of the Ministry of Education, College of Chemistry and Molecular Engineering, Peking University, Beijing 100871, China

## Supporting Information

**ABSTRACT:** Trace vapor detection of hydrogen peroxide ( $\text{H}_2\text{O}_2$ ) represents a practical approach to nondestructive detection of peroxide-based explosives, including liquid mixtures of  $\text{H}_2\text{O}_2$  and fuels and energetic peroxide derivatives, such as triacetone triperoxide (TATP), diacetone diperoxide (DADP), and hexamethylene triperoxide diamine (HMTD). Development of a simple chemical sensor system that responds to  $\text{H}_2\text{O}_2$  vapor with high reliability and sufficient sensitivity (reactivity) remains a challenge. We report a fluorescence ratiometric sensor molecule, diethyl 2,5-bis(((4-(4,4,5,5-tetramethyl-1,3,2-dioxaborolan-2-yl)-benzyl)oxy)carbonyl)amino)terephthalate (DAT-B), for  $\text{H}_2\text{O}_2$

that can be fabricated into an expedient, reliable, and sensitive sensor system suitable for trace vapor detection of  $\text{H}_2\text{O}_2$ . DAT-B is fluorescent in the blue region, with an emission maximum at 500 nm in the solid state. Upon reaction with  $\text{H}_2\text{O}_2$ , DAT-B is converted to an electronic “push–pull” structure, diethyl 2,5-diaminoterephthalate (DAT-N), which has an emission peak at a longer wavelength centered at 574 nm. Such  $\text{H}_2\text{O}_2$ -mediated oxidation of aryl boronates can be accelerated through the addition of an organic base such as tetrabutylammonium hydroxide (TBAH), resulting in a response time of less than 0.5 s under 1 ppm of  $\text{H}_2\text{O}_2$  vapor. The strong overlap between the absorption band of DAT-N and the emission band of DAT-B enables efficient Förster resonance energy transfer (FRET), thus allowing further enhancement of the sensing efficiency of  $\text{H}_2\text{O}_2$  vapor. The detection limit of a drop-cast DAT-B/TBAH film was projected to be 7.7 ppb. By combining high sensitivity and selectivity, the reported sensor system may find broad application in vapor detection of peroxide-based explosives and relevant chemical reagents through its fabrication into easy-to-use, cost-effective kits.

**KEYWORDS:** vapor detection, hydrogen peroxide, fluorescent sensor, FRET



## INTRODUCTION

Development of simple, cost-effective, and sensitive sensor systems to approach trace explosive detection becomes more critical with increasing concern over homeland security and military operational safety as well as environmental and industrial concerns.<sup>1–5</sup> Of the explosive detection methods developed thus far, vapor detection has proven to be one of the practical, nondestructive ways suitable for both trace and bulk explosive monitoring.<sup>6–20</sup> Several methods have been applied to developing novel vapor detection systems for explosives, including fluorescence spectroscopy,<sup>6,9,19,21–23</sup> colorimetry,<sup>14,16,24,25</sup> ion mobility spectrometry (IMS),<sup>26–29</sup> and electrochemical methods.<sup>7,10,30–32</sup> Among the current vapor detection technologies, fluorescence spectroscopy is superior in its simple operation system, fast response, and high sensitivity.

Recently, fluorescence “turn-on” molecular sensors have drawn increasing attention for explosive detection in both the liquid and gas phases.<sup>19,21,33–35</sup> However, the influence of sensor concentration, local environment, and excitation intensity on fluorescence enhancement has limited the

development of these molecular sensors.<sup>36</sup> In general, these challenges can be overcome by the exploitation of ratiometric fluorescence sensors via Förster resonance energy transfer (FRET) between the pristine and reacted sensor molecules. FRET is a fundamental photophysical process and is widely used for developing ion sensors,<sup>37–39</sup> pH sensors,<sup>40–42</sup> and explosive sensors<sup>33,43–46</sup> in solution because of the ability of FRET to enhance the sensitivity and reliability of these sensors.<sup>47</sup> The employment of energy transfer can benefit from dual emission wavelength monitoring to improve the reliability and to reduce the background noise to improve the sensitivity. However, there are few reports on the FRET-based fluorescent sensors for vapor detection.

Peroxide explosives (e.g., triacetone triperoxide (TATP), diacetone diperoxide (DADP), and hexamethylene triperoxide diamine (HMTD)) can be easily made from commercially

Received: March 13, 2014

Accepted: May 7, 2014

Published: May 7, 2014

available products, and they represent one class of the most elusive explosives. However, development of efficient sensors toward these explosives has been hindered because of the lack of a nitro group, the nonfluorescence, and the minimal UV–vis absorption of these explosive compounds.<sup>3,48</sup> Hydrogen peroxide ( $\text{H}_2\text{O}_2$ ) is typically taken as a signature compound for peroxide-based explosives,<sup>48,49</sup> which comes from either the impurity of the explosives (as starting material) or the UV decomposition of peroxides. An appropriate trace vapor detection method for  $\text{H}_2\text{O}_2$  will facilitate security monitoring.<sup>50</sup> There are various reports on the detection of  $\text{H}_2\text{O}_2$  vapor, for example, using electrochemical,<sup>30,31</sup> colorimetric,<sup>14,16</sup> and fluorimetric<sup>19,21,22</sup> methods. However, the vapor detection of  $\text{H}_2\text{O}_2$  at trace levels (e.g., ppb) remains challenging, mainly because of the combined difficulty of molecular design and materials engineering to produce a sensor system that not only features strong binding with  $\text{H}_2\text{O}_2$  (for efficient vapor sampling) but also an expedient, selective reaction with  $\text{H}_2\text{O}_2$  to transduce a readable signal. Although there are a few recent papers reporting fluorescent vapor sensors for  $\text{H}_2\text{O}_2$ ,<sup>21,22</sup> the stoichiometric response and single channel output limit their improved sensitivity and reliability. There is a critical need to develop a simple, expedient, reliable fluorescence sensor system that can detect  $\text{H}_2\text{O}_2$  vapor, ideally down to a few parts per billion.

## MATERIALS AND GENERAL METHODS

4-(Hydroxymethyl)phenylboronic acid pinacol ester, triphosgene, and 4-dimethylaminopyridine (DMAP) were purchased from Sigma-Aldrich and used as received. All solvents were purchased from the manufacturer and used as received unless otherwise noted.

UV–vis absorption spectra were measured on a PerkinElmer Lambda 25 spectrophotometer or an Agilent Cary 100. The fluorescence spectra were measured on a PerkinElmer LS 55 spectrophotometer or an Agilent Eclipse spectrophotometer.  $^1\text{H}$  and  $^{13}\text{C}$  NMR spectra were recorded on a Varian Unity 300 MHz spectrometer at room temperature in appropriate deuterated solvents. All chemical shifts are reported in parts per million (ppm). ESI-HRMS spectra were recorded on a Micromass Quattro II triple quadrupole mass spectrometer, and the solvent used was methanol. All FTIR spectra were collected by Magna IR 750 spectrometer (Nicolet Company) with a resolution of  $1\text{ cm}^{-1}$ , and 100 scans were accumulated to obtain an acceptable S/N ratio; the samples were prepared with KBr pellets. The wavenumber range recorded was  $400\text{--}3900\text{ cm}^{-1}$ .

The synthetic route for sensor molecule DAT-B and the possible mechanism of the reaction between DAT-B and  $\text{H}_2\text{O}_2$  are shown in Scheme S1.

Diethyl 2,5-diaminoterephthalate (2, DAT-N). DAT-N was synthesized according to a literature procedure.<sup>51</sup>  $^1\text{H}$  NMR ( $\text{CDCl}_3$ , 300 MHz, ppm):  $\delta$  7.25 (2 H, s, Ar-H), 4.31–4.38 (4 H, q,  $\text{CH}_2$ ), 1.37–1.42 (6 H, t,  $\text{CH}_3$ ).

Diethyl 2,5-bis((4-(4,4,5,5-tetramethyl-1,3,2-dioxaborolan-2-yl)-benzyloxy)carbonylamino)terephthalate (3, DAT-B). DAT-B was synthesized following the method previously reported to synthesize a similar compound.<sup>52</sup> Triphosgene solution (58.8 mg, 0.198 mmol in 5 mL of anhydrous toluene) was added dropwise to a mixture solution (4 mL of anhydrous toluene) of DAT-N (50 mg, 0.198 mmol) and DMAP (72.6 mg, 0.595 mmol). This mixed solution was heated to reflux for 3 h. After cooling to room temperature, the reaction mixture was diluted with 6 mL of anhydrous  $\text{CH}_2\text{Cl}_2$  and filtered. The filtrate was added the boronated benzyl alcohol (51 mg, 0.218 mmol) and stirred at room temperature for an additional 3 h. The reaction was then concentrated and purified by flash column chromatography (silica gel,  $\text{CHCl}_3/\text{MeOH}$ ). The product was obtained as light yellow powder (42 mg, 27.4%).  $^1\text{H}$  NMR (Figure S1,  $\text{CDCl}_3$ , 300 MHz, ppm):  $\delta$  10.35 (2 H, s, NH), 9.07 (2 H, s, Ar-H), 7.81–7.84 (4 H, d, Ar-H),

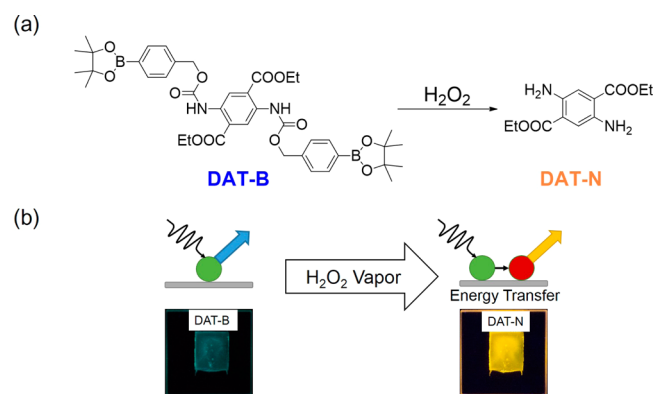
7.41–7.43 (4 H, d, Ar-H), 5.24 (4 H, s,  $\text{CH}_2$ ), 4.37–4.44 (4 H, q,  $\text{CH}_2$ ), 1.40–1.44 (6 H, t,  $\text{CH}_3$ ), 1.34 (24 H, s,  $\text{CH}_3$ ).  $^{13}\text{C}$  NMR (Figure S2,  $\text{CDCl}_3$ , 75 MHz, ppm):  $\delta$  167.2, 153.4, 139.0, 135.0, 135.0, 127.2, 121.1, 119.8, 83.8, 77.4, 47.0, 76.6, 66.7, 62.6, 24.8, 14.1. ESI-HRMS  $m/z$ :  $[\text{M} + \text{H}]^+$  calcd, 772.3550; found, 773.3628.

The vapor sensing tests were performed with thin films of DAT-B deposited on quartz slides. Briefly, 25  $\mu\text{L}$  of an ethanol solution of DAT-B at different concentrations (also containing appropriate concentrations of TBAH as indicated) was drop-cast uniformly onto a  $2.5 \times 2.5\text{ cm}^2$  quartz slide to form a  $1.0 \times 1.0\text{ cm}^2$  solid film (guided by Scotch tape) followed by drying at room temperature in vacuum for 1 h. The optimum molar amount of DAT-B was determined to be 0.25  $\mu\text{mol}$ , as shown in Figure S3.

## RESULTS AND DISCUSSION

Herein, we present a fluorescent ratiometric sensor, diethyl 2,5-bis(((4-(4,4,5,5-tetramethyl-1,3,2-dioxaborolan-2-yl)benzyl)-oxy)carbonylamino)terephthalate (DAT-B), for  $\text{H}_2\text{O}_2$  (Scheme 1) that enables efficient FRET between the pristine

**Scheme 1.** (a) Chemical Reaction between the Sensor Molecule (DAT-B) and  $\text{H}_2\text{O}_2$ , Leading to the Formation of DAT-N; (b) Illustration Showing the Intrinsic Fluorescence Emission of DAT-B and the FRET Process between DAT-B and DAT-N<sup>a</sup>



<sup>a</sup>Photographs at the bottom of panel b show the fluorescence emission change of the DAT-B film deposited on a quartz slide (0.25  $\mu\text{mol}$  DAT-B and 1.25  $\mu\text{mol}$  TBAH,  $1.0 \times 1.0\text{ cm}^2$ ) after exposure to 225 ppm of  $\text{H}_2\text{O}_2$  for 5 min.

and reacted states in solid films and serves as a highly sensitive and selective sensor for  $\text{H}_2\text{O}_2$  vapor. The sensing mechanism lies in the oxidation of the boronate group of DAT-B, resulting in turning on the intramolecular charge-transfer (ICT) band at longer wavelengths (Figure S4).<sup>53</sup> This fluorescent molecule has a blue emission centered at 500 nm in a drop-cast film (Scheme 1b), which is attributed to the central  $\pi$ -conjugation of DAT-B. Upon reaction with  $\text{H}_2\text{O}_2$ , the aryl boronate group in DAT-B is transformed to a phenol group followed by a rearrangement of the side benzene group, producing an amino group at the core (Figure S5). The product thus formed, diethyl 2,5-diaminoterephthalate (DAT-N), has an electron donor–acceptor (“push–pull”) structure. The formation of a push–pull structure turns on the ICT transition (i.e., fluorescent emission in the longer wavelength band;  $\lambda_{\text{max}}$  at 574 nm). This new, red-shifted emission makes DAT-B a suitable ratiometric fluorescence sensor for  $\text{H}_2\text{O}_2$  detection.<sup>54</sup> The two emission bands at 500 and 574 nm can be monitored concurrently to measure the FRET process between DAT-B and DAT-N. Such dual band monitoring will enhance

the detection reliability, whereas the FRET measurement will further increase the detection efficiency (Figure 2).

Recent work has shown that various functionalized DAT-N derivatives containing only one benzene ring as the aromatic component serve as novel fluorophores and emit intense visible light with excellent quantum yields (>90%) in the solid state.<sup>55</sup> Taking advantage of the push–pull structure, the emission colors can be tuned in the range from blue to red simply by modifying the side chain substituents.<sup>55–57</sup> The combination of the high-solid-state quantum yield and facile structure modification is highly conducive to the development of solid-state sensors that can be tuned to afford efficient FRET to further enhance the detection efficiency. The boronate group was chosen to functionalize DAT-B because of its highly selective reaction with  $\text{H}_2\text{O}_2$ .<sup>53</sup> Moreover, the strong electron-withdrawing capability of the amide group weakens the electron-donating strength of the amino group, thus blocking the ICT transition with DAT-B.

The  $\text{H}_2\text{O}_2$  mediated oxidation of boronate (shown in Scheme 1a) was investigated in detail through both UV–vis absorption and fluorescence spectral measurements of DAT-B and DAT-N in drop-cast films. As shown in Figure 1, the main

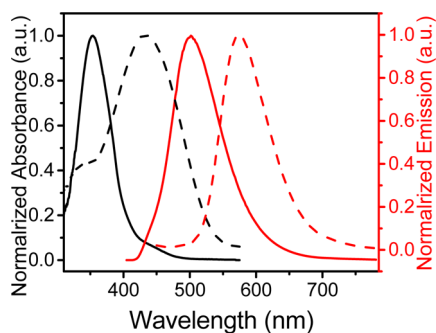


**Figure 1.** Absorption (black) and fluorescence (red) spectra of a DAT-B film ( $0.25 \mu\text{mol}$  of DAT-B blended with  $1.25 \mu\text{mol}$  of TBAH,  $1.0 \times 1.0 \text{ cm}^2$ ) deposited on quartz slides before (solid lines) and after (dashed lines) exposure to  $\text{H}_2\text{O}_2$  vapor (225 ppm, 15 min).

absorption of the reaction product, DAT-N, shifts to a longer wavelength by ca. 103 nm. This red-shifted absorption band corresponds to the ICT transition between the amino groups and carbonyl modified  $\pi$ -conjugation core. The conversion from an electron-accepting group (amide) to an electron-donating group (amino) renders formation of a push–pull structure in the molecule, which results in an ICT transition located at the longer wavelength absorption.<sup>22</sup> Before reacting with  $\text{H}_2\text{O}_2$ , the drop-cast film of DAT-B mixed with tetrabutylammonium hydroxide (TBAH) emits a blue emission centered at 500 nm, which is attributed to the  $\pi$ – $\pi^*$  transition of the molecule's core. The significant spectral overlap between the absorption of DAT-N (acceptor) and the emission of DAT-B (donor) enables FRET between the two molecules. When cast in a solid film, the short distance between the molecules may produce a high efficiency of FRET, which can in turn enhance the sensing sensitivity, as discussed later. Because of the intrinsic reaction specificity of the boronate group with  $\text{H}_2\text{O}_2$ , the sensor molecule, DAT-B, demonstrated no obvious fluorescence shifts or quenching upon exposure to the vapor of water or to common organic reagents such as alcohols, hexane, acetone, and others (Figure S6).

The reaction speed of the  $\text{H}_2\text{O}_2$ -mediated oxidation of aryl boronates was greatly accelerated by the addition of a base, which assists the formation of  $\text{HO}_2^-$  anion (acting as a nucleophile) from  $\text{H}_2\text{O}_2$  and then reacts with the boronate group (a strong electrophile).<sup>54</sup> We chose TBAH as the base to produce both the basic conditions needed for the oxidation reaction and a hydrophilic film surface for efficient condensation of  $\text{H}_2\text{O}_2$  vapor (Figure S7). The DAT-B/TBAH film shows minimal spectral changes compared to that of the pure DAT-B film within at least 7 days, which proves the stability of the composite film (Figure S8). The optimal molar ratio of TBAH to DAT-B in the composite film was determined to be 5:1, regarding both the reaction speed and the total amount of DAT-B converted (Figure S9). Less TBAH gives incomplete oxidation of  $\text{H}_2\text{O}_2$ , and excess TBAH decreases the surface concentration of DAT-B molecules.

To demonstrate the efficient FRET between the sensor molecule, DAT-B, and its reaction product, DAT-N, systematic absorption and emission spectral measurements of DAT-B/TBAH films were performed as shown in Figure 2. Figure 2a shows the spectra of the DAT-B/TBAH film after being exposed to 500 ppb of  $\text{H}_2\text{O}_2$  vapor and is compared to the spectra recorded over the directly blended DAT-B/DAT-N/TBAH film. Upon exposure to  $\text{H}_2\text{O}_2$  vapor, the major absorption peak of DAT-B at 353 nm decreases by about 13% along with an increase in the region around 420 nm. In contrast, the emission intensity of DAT-B at the main peak (500 nm) decreases by more than 75%, along with a new emission band that emerges at a longer wavelength. This large fluorescence quenching of DAT-B cannot be explained by the stoichiometric reaction, which otherwise should be around 13%, as indicated by the absorption measurement. The greatly enhanced quenching efficiency is attributed to FRET between the pristine DAT-B molecule and the reaction product, DAT-N.

To confirm the occurrence of FRET in the film further, we prepared a film with DAT-B directly blended with DAT-N (molar ratio of DAT-B/DAT-N = 9:1) and measured the absorption and emission spectra. Consistent with the 10% decrease in concentration of DAT-B in the blended film, the absorption at the 353 nm peak was decreased by about the same percentage (Figure 2c). However, the emission intensity of DAT-B was decreased by more than 80% compared to that of the DAT-B film without DAT-N. This extending of fluorescence quenching is 8 times larger than the percentage of the concentration decrease of DAT-B, clearly indicating the existence of a FRET quenching process between DAT-B and DAT-N. Such FRET-based amplification of fluorescence quenching has been utilized in sensing applications, which has been proven to effectively lower the detection limit.<sup>43</sup> However, a similar quenching amplification has rarely been applied in vapor detection systems, for which the major technical challenge lies in the molecular design and materials engineering that afford both efficient FRET and a suitable interface for the effective collection of analyte molecules. It would be interesting to compare the fluorescence quenching data shown in Figure 2b,d. Considering the comparable extent of the emission intensity's decrease in the two cases (both about 80%), we argue that the concentration of DAT-N produced in Figure 2b upon exposure to  $\text{H}_2\text{O}_2$  vapor should be approximately the same as that blended in the film in Figure 2d (i.e.,  $0.025 \mu\text{mol}$ ). This corresponds to only 10% of DAT-B (initially  $0.25 \mu\text{mol}$ ) converted to DAT-N, although this small

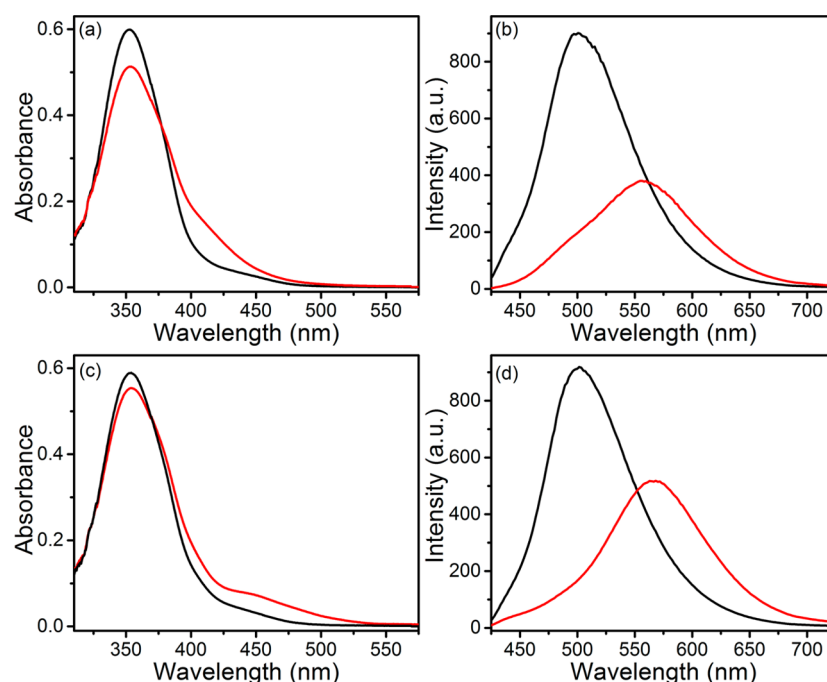


**Figure 2.** Absorption (a) and fluorescence (b) spectra of a pristine DAT-B film (black) and the same film after exposure to 500 ppb of H<sub>2</sub>O<sub>2</sub> vapor for 360 s (red) (0.25  $\mu$ mol of DAT-B and 1.25  $\mu$ mol of TBAH). Absorption (c) and fluorescence (d) spectra of DAT-B (black, 0.25  $\mu$ mol of DAT-B and 1.25  $\mu$ mol of TBAH) and the DAT-B/DAT-N blended film (red, 0.225  $\mu$ mol of DAT-B, 0.025  $\mu$ mol of DAT-N, and 1.25  $\mu$ mol of TBAH). All films were deposited to form a 1.0  $\times$  1.0 cm<sup>2</sup> square on quartz slides and were excited at 353 nm.

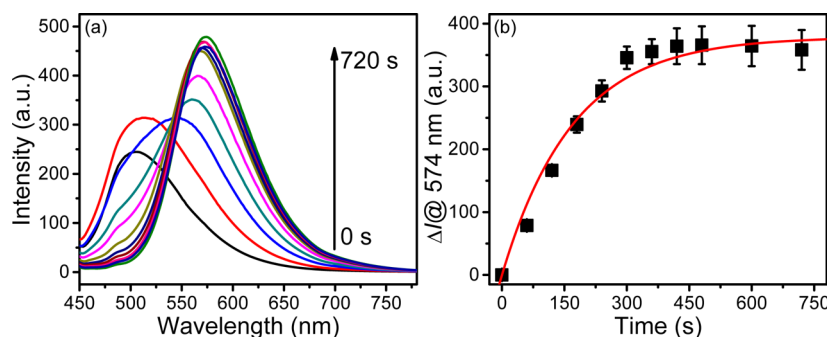


**Figure 3.** Fluorescence spectra of DAT-B coated on a 1.0  $\times$  1.0 cm<sup>2</sup> quartz slide (containing 0.25  $\mu$ mol of DAT-B and 1.25  $\mu$ mol of TBAH) recorded at various time intervals after exposure to 1 ppm of H<sub>2</sub>O<sub>2</sub> vapor ( $\lambda_{\text{ex}} = 427$  nm). (b) Emission intensity increase,  $\Delta I$ , measured at 574 nm ( $\lambda_{\text{ex}} = 427$  nm) as a function of exposure time, for which the data points are fitted following a first-order surface reaction between DAT-B and H<sub>2</sub>O<sub>2</sub> (see the Supporting Information for detail of the kinetics fitting). The error bars are based on the standard deviations of the measured emission intensities.

fraction of conversion generates a fluorescence quenching as large as 80%. Using a well-calibrated fluorometer, we can measure a 1% decrease in emission intensity, meaning only a 0.1% conversion of DAT-B within the thin film. This will enable us to significantly shorten the sensor response time under the same vapor pressure level of H<sub>2</sub>O<sub>2</sub>.

The fluorescence spectral change of the DAT-B film was also investigated by exposing it to 1 ppm of H<sub>2</sub>O<sub>2</sub> vapor for different time intervals to demonstrate the response speed of this sensor system. The reaction was monitored by measuring the fluorescence emission of DAT-N. As shown in Figure 3, the fluorescence emission peak at 574 nm increases gradually with exposure time (corresponding to the generation of DAT-N), and at the same time, the emission peak at 500 nm (corresponding to the consumption of DAT-B) gradually decreases. The reaction kinetics plotted as the emission intensity increase versus the exposure time (shown in Figure

3b) are fitted to a pseudo-first-order reaction kinetic.<sup>58</sup> Three times the standard deviation ( $\sigma = 0.9$ ) of the noise floor was set as the threshold of a detectable emission level. The corresponding response time for this sensor system obtained from the fitted data in Figure 3b is less than 0.5 s. Such rapid response toward H<sub>2</sub>O<sub>2</sub> vapor meets the urgent need of real-time in-field detection of peroxide-based explosives. This expedient sensor response toward low concentrations of H<sub>2</sub>O<sub>2</sub> vapor (as low as 1 ppm) is likely due to the surface properties of the film, which are conducive to fast sampling of hydrophilic gas analytes.

To explore the advantage of this DAT-B sensor system further, the optimal sensor composite of DAT-B (blended with TBAH within a drop-cast film) was expected to afford a competitive detection limit. To determine the detection limit of this system, the DAT-B composite was exposed for 10 min to the vapor of an aqueous solution of H<sub>2</sub>O<sub>2</sub> at various

concentrations (which correspondingly provides different vapor pressures of H<sub>2</sub>O<sub>2</sub>),<sup>59</sup> and the increases in the fluorescence intensity at 574 nm (relative to the value measured under pure water vapor) were recorded. The fluorescence intensity increases with the H<sub>2</sub>O<sub>2</sub> vapor pressure (Figure 4). Assuming

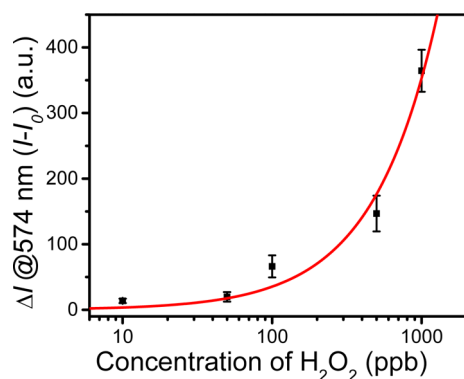


**Figure 4.** Plot showing the fluorescence intensity increase ( $\Delta I$ ) measured at 574 nm ( $\lambda_{\text{ex}} = 427$  nm) as a function of the vapor pressure of H<sub>2</sub>O<sub>2</sub>, for which the data points are fitted following the Langmuir adsorption model (see the Supporting Information). The error bars are based on the standard deviations of the measured emission intensities.

that a quasi-equilibrium was reached within 10 min of exposure (as implied by the result in Figure 3b), the results shown in Figure 4 follow the Langmuir adsorption model (see the Supporting Information). After fitting the experimental data into the Langmuir equation, the detection limit of this sensor system is projected to be 7.7 ppb by defining an intensity increase of 3 times the standard deviation as the detectable signal. It should be noted that such high detection sensitivity (about 2 orders of magnitude better than a commercial fluorescence detector) was obtained simply through a drop-cast film. Further improvement in the sensitivity can be achieved by spin-casting the sensor material into an optical tube coupled to a photodetector, as previously demonstrated by Swager et al. with the Fido detector system.<sup>60</sup>

## CONCLUSIONS

We have developed an expedient fluorescence ratiometric sensor system for trace vapor detection of H<sub>2</sub>O<sub>2</sub>. The sensing mechanism is based on H<sub>2</sub>O<sub>2</sub>-mediated oxidation of a boronate fluorophore, DAT-B, which is then converted to an amino-substituted product, DAT-N. The emission of the DAT-B film is blue (centered at 500 nm), whereas the emission of DAT-N within the same film is significantly red-shifted to 574 nm. The red-shifted emission band is due to the ICT band of DAT-N. The spectral overlap of the DAT-B emission and DAT-N absorption bands results in an efficient FRET process, which can be exploited to enhance the sensor performance in terms of both sensitivity and response speed. Considering the over 70 nm separation between the emission bands of DAT-B and DAT-N, the sensor system thus developed will also be well-suited for dual channel (wavelength) monitoring to enhance the reliability of detection, particularly when compared to that of conventional fluorescence sensors based on single wavelength monitoring (quenching or turn-on). By blending the DAT-B sensor with a hydrophilic organic base at the appropriate molar ratio, the sensor composite demonstrated effective vapor sampling (absorption) of H<sub>2</sub>O<sub>2</sub>, resulting in

both high detection sensitivity (down to 7.7 ppb) and fast sensor response (down to 0.5 s under 1 ppm of H<sub>2</sub>O<sub>2</sub>). The exploitation of FRET in solid films broadens the development of sensors for trace vapor detection, providing great potential for improving the detection limit.

## ASSOCIATED CONTENT

### Supporting Information

Proposed sensing mechanism; NMR spectra of DAT-B; optimization of film preparation; absorbance and fluorescence spectra of DAT-B and DAT-N in solution; IR spectra of DAT-B and DAT-N; selectivity test; contact angle measurements; stability test; and data fitting. This material is available free of charge via the Internet at <http://pubs.acs.org>.

## AUTHOR INFORMATION

### Corresponding Author

\*E-mail: [lzang@eng.utah.edu](mailto:lzang@eng.utah.edu).

### Author Contributions

<sup>§</sup>M.X. and J.-M.H. contributed equally to this work.

### Notes

The authors declare no competing financial interest.

## ACKNOWLEDGMENTS

This work was supported by DHS (2009-ST-108-LR0005). We thank Benjamin R. Bunes for proof reading the manuscript.

## REFERENCES

- (1) Toal, S. J.; Trogler, W. C. Polymer Sensors for Nitroaromatic Explosives Detection. *J. Mater. Chem.* **2006**, *16*, 2871–2883.
- (2) Thomas, S. W.; Joly, G. D.; Swager, T. M. Chemical Sensors Based on Amplifying Fluorescent Conjugated Polymers. *Chem. Rev.* **2007**, *107*, 1339–1386.
- (3) Wang, J. Electrochemical Sensing of Explosives. *Electroanalysis* **2007**, *19*, 415–423.
- (4) Moore, D. Recent Advances in Trace Explosives Detection Instrumentation. *Sens. Imaging* **2007**, *8*, 9–38.
- (5) Germain, M. E.; Knapp, M. J. Optical Explosives Detection: From Color Changes to Fluorescence Turn-On. *Chem. Soc. Rev.* **2009**, *38*, 2543–2555.
- (6) Yang, J.-S.; Swager, T. M. Fluorescent Porous Polymer Films as TNT Chemosensors: Electronic and Structural Effects. *J. Am. Chem. Soc.* **1998**, *120*, 11864–11873.
- (7) Staii, C.; Johnson, A. T.; Chen, M.; Gelperin, A. DNA-Decorated Carbon Nanotubes for Chemical Sensing. *Nano Lett.* **2005**, *5*, 1774–1778.
- (8) Johnson, A. T. C.; Staii, C.; Chen, M.; Khamis, S.; Johnson, R.; Klein, M. L.; Gelperin, A. DNA-Decorated Carbon Nanotubes for Chemical Sensing. *Phys. Status Solidi B* **2006**, *243*, 3252–3256.
- (9) Naddo, T.; Che, Y.; Zhang, W.; Balakrishnan, K.; Yang, X.; Yen, M.; Zhao, J.; Moore, J. S.; Zang, L. Detection of Explosives with a Fluorescent Nanofibril Film. *J. Am. Chem. Soc.* **2007**, *129*, 6978–6979.
- (10) Bohrer, F. I.; Colesniuc, C. N.; Park, J.; Schuller, I. K.; Kummel, A. C.; Trogler, W. C. Selective Detection of Vapor Phase Hydrogen Peroxide with Phthalocyanine Chemiresistors. *J. Am. Chem. Soc.* **2008**, *130*, 3712–3713.
- (11) Zyryanov, G. V.; Palacios, M. A.; Anzenbacher, P. Simple Molecule-Based Fluorescent Sensors for Vapor Detection of TNT. *Org. Lett.* **2008**, *10*, 3681–3684.
- (12) Díaz Aguilar, A.; Forzani, E. S.; Leright, M.; Tsow, F.; Cagan, A.; Iglesias, R. A.; Nagahara, L. A.; Amlani, I.; Tsui, R.; Tao, N. J. A Hybrid Nanosensor for TNT Vapor Detection. *Nano Lett.* **2009**, *10*, 380–384.
- (13) Tenhaeff, W. E.; McIntosh, L. D.; Gleason, K. K. Synthesis of Poly(4-vinylpyridine) Thin Films by Initiated Chemical Vapor

Deposition (ICVD) for Selective Nanotrench-Based Sensing of Nitroaromatics. *Adv. Funct. Mater.* **2010**, *20*, 1144–1151.

(14) Lin, H.; Suslick, K. S. A Colorimetric Sensor Array for Detection of Triacetone Triperoxide Vapor. *J. Am. Chem. Soc.* **2010**, *132*, 15519–15521.

(15) Zhang, C.; Che, Y.; Yang, X.; Bunes, B. R.; Zang, L. Organic Nanofibrils Based on Linear Carbazole Trimer for Explosive Sensing. *Chem. Commun.* **2010**, *46*, 5560–5562.

(16) Xu, M.; Bunes, B. R.; Zang, L. Paper-Based Vapor Detection of Hydrogen Peroxide: Colorimetric Sensing with Tunable Interface. *ACS Appl. Mater. Interfaces* **2011**, *3*, 642–647.

(17) Kartha, K. K.; Babu, S. S.; Srinivasan, S.; Ajayaghosh, A. Attogram Sensing of Trinitrotoluene with a Self-Assembled Molecular Gelator. *J. Am. Chem. Soc.* **2012**, *134*, 4834–4841.

(18) Che, Y.; Gross, D. E.; Huang, H.; Yang, D.; Yang, X.; Discekici, E.; Xue, Z.; Zhao, H.; Moore, J. S.; Zang, L. Diffusion-Controlled Detection of Trinitrotoluene: Interior Nanoporous Structure and Low Highest Occupied Molecular Orbital Level of Building Blocks Enhance Selectivity and Sensitivity. *J. Am. Chem. Soc.* **2012**, *134*, 4978–4982.

(19) Zheng, J. Y.; Yan, Y.; Wang, X.; Shi, W.; Ma, H.; Zhao, Y. S.; Yao, J. Hydrogen Peroxide Vapor Sensing with Organic Core/Sheath Nanowire Optical Waveguides. *Adv. Mater.* **2012**, *24*, OP194–OP199.

(20) Grate, J. W.; Ewing, R. G.; Atkinson, D. A. Vapor-Generation Methods for Explosives-Detection Research. *TrAC, Trends Anal. Chem.* **2012**, *41*, 1–14.

(21) Sanchez, J. C.; Trogler, W. C. Polymerization of a Boronate-Functionalized Fluorophore by Double Transesterification: Applications to Fluorescence Detection of Hydrogen Peroxide Vapor. *J. Mater. Chem.* **2008**, *18*, 5134–5141.

(22) Xu, M.; Han, J.-M.; Zhang, Y.; Yang, X.; Zang, L. A Selective Fluorescence Turn-On Sensor for Trace Vapor Detection of Hydrogen Peroxide. *Chem. Commun.* **2013**, *49*, 11779–11781.

(23) Gopalakrishnan, D.; Dichtel, W. R. Direct Detection of RDX Vapor Using a Conjugated Polymer Network. *J. Am. Chem. Soc.* **2013**, *135*, 8357–8362.

(24) Bernasconi, C. F. Kinetic and Spectral Study of Some Reactions of 2,4,6-Trinitrotoluene in Basic Solution. I. Deprotonation and Janovsky Complex Formation. *J. Org. Chem.* **1971**, *36*, 1671–1679.

(25) Forzani, E. S.; Lu, D.; Leright, M. J.; Aguilar, A. D.; Tsow, F.; Iglesias, R. A.; Zhang, Q.; Lu, J.; Li, J.; Tao, N. A Hybrid Electrochemical–Colorimetric Sensing Platform for Detection of Explosives. *J. Am. Chem. Soc.* **2009**, *131*, 1390–1391.

(26) McGann, W.; Haigh, P.; Neves, J. L. Expanding the Capability of IMS Explosive Trace Detection. *Int. J. Ion Mobility Spectrom.* **2002**, *5*, 119–122.

(27) Tam, M.; Hill, H. H. Secondary Electrospray Ionization-Ion Mobility Spectrometry for Explosive Vapor Detection. *Anal. Chem.* **2004**, *76*, 2741–2747.

(28) Oxley, J. C.; Smith, J. L.; Kirschenbaum, L. J.; Marimganti, S.; Vadlamannati, S. Detection of Explosives in Hair Using Ion Mobility Spectrometry. *J. Forensic Sci.* **2008**, *53*, 690–693.

(29) Najarro, M.; Davila Morris, M. E.; Staymates, M. E.; Fletcher, R.; Gillen, G. Optimized Thermal Desorption for Improved Sensitivity in Trace Explosives Detection by Ion Mobility Spectrometry. *Analyst* **2012**, *137*, 2614–2622.

(30) Benedet, J.; Lu, D. L.; Cizek, K.; La Belle, J.; Wang, J. Amperometric Sensing of Hydrogen Peroxide Vapor for Security Screening. *Anal. Bioanal. Chem.* **2009**, *395*, 371–376.

(31) Komkova, M. A.; Karyakina, E. E.; Marken, F.; Karyakin, A. A. Hydrogen Peroxide Detection in Wet Air with a Prussian Blue Based Solid Salt Bridged Three Electrode System. *Anal. Chem.* **2013**, *85*, 2574–2577.

(32) Schnorr, J. M.; van der Zwaag, D.; Walish, J. J.; Weizmann, Y.; Swager, T. M. Sensory Arrays of Covalently Functionalized Single-Walled Carbon Nanotubes for Explosive Detection. *Adv. Funct. Mater.* **2013**, *23*, 5285–5291.

(33) Freeman, R.; Finder, T.; Bahshi, L.; Gill, R.; Willner, I. Functionalized CdSe/ZnS QDs for the Detection of Nitroaromatic or RDX Explosives. *Adv. Mater.* **2012**, *24*, 6416–6421.

(34) Andrew, T. L.; Swager, T. M. Detection of Explosives via Photolytic Cleavage of Nitroesters and Nitramines. *J. Org. Chem.* **2011**, *76*, 2976–2993.

(35) Ma, H.; Gao, R.; Yan, D.; Zhao, J.; Wei, M. Organic–Inorganic Hybrid Fluorescent Ultrathin Films and Their Sensor Application for Nitroaromatic Explosives. *J. Mater. Chem. C* **2013**, *1*, 4128–4137.

(36) Yuan, L.; Lin, W.; Zheng, K.; Zhu, S. FRET-Based Small-Molecule Fluorescent Probes: Rational Design and Bioimaging Applications. *Acc. Chem. Res.* **2013**, *46*, 1462–1473.

(37) Zhou, Z.; Yu, M.; Yang, H.; Huang, K.; Li, F.; Yi, T.; Huang, C. FRET-Based Sensor for Imaging Chromium(III) in Living Cells. *Chem. Commun.* **2008**, 3387–3389.

(38) Yu, H.; Fu, M.; Xiao, Y. Switching Off FRET by Analyte-Induced Decomposition of Squaraine Energy Acceptor: A Concept to Transform ‘Turn Off’ Chemodosimeter into Ratiometric Sensors. *Phys. Chem. Chem. Phys.* **2010**, *12*, 7386–7391.

(39) Yu, H.; Xiao, Y.; Guo, H.; Qian, X. Convenient and Efficient FRET Platform Featuring a Rigid Biphenyl Spacer between Rhodamine and Bodipy: Transformation of ‘Turn-On’ Sensors into Ratiometric Ones with Dual Emission. *Chem.—Eur. J.* **2011**, *17*, 3179–3191.

(40) Snee, P. T.; Somers, R. C.; Nair, G.; Zimmer, J. P.; Bawendi, M. G.; Nocera, D. G. A Ratiometric CdSe/ZnS Nanocrystal pH Sensor. *J. Am. Chem. Soc.* **2006**, *128*, 13320–13321.

(41) Jin, T.; Sasaki, A.; Kinjo, M.; Miyazaki, J. A Quantum Dot-Based Ratiometric pH Sensor. *Chem. Commun.* **2010**, *46*, 2408–2410.

(42) Peng, H.-s.; Stolwijk, J. A.; Sun, L.-N.; Wegener, J.; Wolfbeis, O. S. A Nanogel for Ratiometric Fluorescent Sensing of Intracellular pH Values. *Angew. Chem.* **2010**, *122*, 4342–4345.

(43) Freeman, R.; Willner, I. NAD<sup>+</sup>/NADH-Sensitive Quantum Dots: Applications To Probe NAD<sup>+</sup>-Dependent Enzymes and To Sense the RDX Explosive. *Nano Lett.* **2008**, *9*, 322–326.

(44) Freeman, R.; Gill, R.; Shweky, I.; Kotler, M.; Banin, U.; Willner, I. Biosensing and Probing of Intracellular Metabolic Pathways by NADH-Sensitive Quantum Dots. *Angew. Chem., Int. Ed.* **2009**, *48*, 309–313.

(45) Zhang, K.; Zhou, H.; Mei, Q.; Wang, S.; Guan, G.; Liu, R.; Zhang, J.; Zhang, Z. Instant Visual Detection of Trinitrotoluene Particulates on Various Surfaces by Ratiometric Fluorescence of Dual-Emission Quantum Dots Hybrid. *J. Am. Chem. Soc.* **2011**, *133*, 8424–8427.

(46) Wang, Y.; La, A.; Bruckner, C.; Lei, Y. FRET- and PET-Based Sensing in a Single Material: Expanding the Dynamic Range of an Ultra-Sensitive Nitroaromatic Explosives Assay. *Chem. Commun.* **2012**, *48*, 9903–9905.

(47) Lakowicz, J. R. *Principles of Fluorescence Spectroscopy*, 2nd ed.; Kluwer Academic/Plenum Publishers: New York, 1999.

(48) Schulte-Ladbeck, R.; Vogel, M.; Karst, U. Recent Methods for the Determination of Peroxide-Based Explosives. *Anal. Bioanal. Chem.* **2006**, *386*, 559–565.

(49) Burks, R.; Hage, D. Current Trends in the Detection of Peroxide-Based Explosives. *Anal. Bioanal. Chem.* **2009**, *395*, 301–313.

(50) Sanchez, J. C.; Trogler, W. C. Efficient Blue-Emitting Silafluorene-Fluorene-Conjugated Copolymers: Selective Turn-Off/Turn-On Detection of Explosives. *J. Mater. Chem.* **2008**, *18*, 3143–3156.

(51) Sinnreich, J. Chemistry of Succinylsuccinic Acid Derivatives. VI. A Specific Synthesis of P-Phenylenediamine. *Synthesis* **1980**, 578–580.

(52) Srikun, D.; Miller, E. W.; Domaille, D. W.; Chang, C. J. An ICT-Based Approach to Ratiometric Fluorescence Imaging of Hydrogen Peroxide Produced in Living Cells. *J. Am. Chem. Soc.* **2008**, *130*, 4596–4597.

(53) Lo, L. C.; Chu, C. Y. Development of Highly Selective and Sensitive Probes for Hydrogen Peroxide. *Chem. Commun.* **2003**, 2728–2729.

(54) Lippert, A. R.; Van de Bittner, G. C.; Chang, C. J. Boronate Oxidation as a Bioorthogonal Reaction Approach for Studying the Chemistry of Hydrogen Peroxide in Living Systems. *Acc. Chem. Res.* **2011**, *44*, 793–804.

(55) Zhao, Y.; Gao, H.; Fan, Y.; Zhou, T.; Su, Z.; Liu, Y.; Wang, Y. Thermally Induced Reversible Phase Transformations Accompanied by Emission Switching between Different Colors of Two Aromatic-Amine Compounds. *Adv. Mater.* **2009**, *21*, 3165–3169.

(56) Zhang, Y.; Starynowicz, P.; Christoffers, J. Fluorescent Bis(oligophenylamino)terephthalates. *Eur. J. Org. Chem.* **2008**, *2008*, 3488–3495.

(57) Shimizu, M.; Takeda, Y.; Higashi, M.; Hiyama, T. 1,4-Bis(Alkenyl)-2,5-dipiperidinobenzenes: Minimal Fluorophores Exhibiting Highly Efficient Emission in the Solid State. *Angew. Chem., Int. Ed.* **2009**, *48*, 3653–3656.

(58) Yuan, L.; Lin, W.; Yang, Y. A Ratiometric Fluorescent Probe for Specific Detection of Cysteine over Homocysteine and Glutathione Based on the Drastic Distinction in the Kinetic Profiles. *Chem. Commun.* **2011**, *47*, 6275–6277.

(59) Manatt, S. L.; Manatt, M. R. R. On the Analyses of Mixture Vapor Pressure Data: The Hydrogen Peroxide/Water System and Its Excess Thermodynamic Functions. *Chem.—Eur. J.* **2004**, *10*, 6540–6557.

(60) Cumming, C. J.; Aker, C.; Fisher, M.; Fok, M.; La Grone, M. J.; Reust, D.; Rockley, M. G.; Swager, T. M.; Towers, E.; Williams, V. Using Novel Fluorescent Polymers as Sensory Materials for Above-Ground Sensing of Chemical Signature Compounds Emanating from Buried Landmines. *IEEE Trans. Geosci. Electron.* **2001**, *39*, 1119–1128.